

Evaluation of Corrosion Inhibition of Aluminum by 2-(4-methylbenzylthio)-3- nitroimidazo [1, 2, a]pyridine in Hydrochloric Acid Medium

Ehouman Ahissan Donatien^{1,*}, Zran Vanh Eric-Simon², Coulibali Siomenan²,
Bamba Amara², Douan Katy Mao², Ablo Evrad², Diabate Massogbè³,
Kouakou Adjoumani Rodrigue¹, Niamien Paulin Marius²

¹Laboratoire de Thermodynamique et Physico-Chimie du Milieu (LTPCM), UFR SFA, Université NANGUI ABROGOUA, Abidjan, Côte-d'Ivoire

²Laboratoire de Constitution et Réaction de la Matière (LCRM), UFR SSMT, Université Félix Houphouët-Boigny, Abidjan Cocody, Abidjan, Côte-d'Ivoire

³Laboratoire de Biochimie Alimentaire et de Technologies des Produits Tropicaux (LBATPT), UFR STA, Université NANGUI ABROGOUA, Abidjan, Côte-d'Ivoire

Abstract Due to its extensive use, the behaviour of aluminium in 1M hydrochloric acid solution was studied in depth in this work. This study which is mainly based on the inhibition properties of 2-(4-methylbenzylthio)-3- nitroimidazo [1, 2, a]pyridine (MTNI) was carried out using the mass loss technique and the theoretical method based on density functional theory (DFT) at the B3LYP level with the base 6-311G (d, p). The inhibitory efficiency of the molecule increases with increasing concentration and decreases with increasing temperature. Adsorption isotherm studies revealed that the molecule adsorbs on the aluminium surface according to the modified Langmuir isotherm or the Villamil isotherm. The Adejo-Ekwenchi isotherm indicates that the adsorption of MTNI is dominated by physisorption. The thermodynamic quantities of adsorption and activation were determined and discussed. The calculated quantum chemical parameters related to the efficiency of inhibition are the energy of the highest occupied molecular orbital E(HOMO), the energy of the lowest unoccupied molecular orbital E(LUMO), the HOMO-LUMO energy gap, the hardness (η), softness (S), dipole moment (μ), electron affinity (A), ionization energy (I), absolute electronegativity (χ), absolute electronegativity (χ), fraction (ΔN) of electrons transferred from MTNI to aluminium and electrophilicity index (ω). The local reactivity was analyzed through the condensed Fukui function and condensed softness indices to determine the nucleophilic and electrophilic attack sites. The theoretical results are consistent with the reported experimental data.

Keywords Corrosion inhibition; aluminium, Density functional theory (DFT), Mass loss method, 2-(4-methylbenzylthio)-3- nitroimidazo [1, 2, a]pyridine

1. Introduction

Pure aluminium is a remarkable metal because it is resistant to corrosion. It is currently the most widely used non-ferrous metal [1] because of its low density and its electrical and thermal performance. It is most often used in industries related to transportation: aviation, automotive, packaging, construction, mechanical, etc. However, when it comes into contact with aggressive media (acids, bases, etc.), its thin protective layer (a few micrometers thick) is destroyed and the material undergoes an alteration (corrosion)

which leads to the loss of its physical and chemical properties. Corrosion results from the chemical or electrochemical action of an environment on metals and alloys. The consequences are important in various fields and in particular in industry: production stoppages, replacement of corroded parts, accidents and pollution risks are frequent situations with sometimes heavy economic consequences [2]. The most effective way of combating this phenomenon is undoubtedly the use of organic molecules (corrosion inhibitors) acting at the metal-environment interface. Several organic molecules have been tested as inhibitors of aluminium corrosion in acidic environments. Thus, hydrazines [3], Schiff bases [4,5], therapeutic molecules [6-9], plant extracts [10-12], etc., have been used successfully.

This work, which is a contribution to the study of

* Corresponding author:

ehoumandona@gmail.com (Ehouman Ahissan Donatien)

Received: Nov. 14, 2021; Accepted: Dec. 6, 2021; Published: Dec. 29, 2021

Published online at <http://journal.sapub.org/ijmc>

corrosion inhibition of metals in acidic media, aims to study the behaviour of 2-(4-methylbenzylthio)-3-nitroimidazo [1, 2, a] pyridine (MTNI) towards the corrosion of aluminium in 1M hydrochloric acid.

2. Experimental Details

2.1. Materials and Sample Preparation

The molecule used as an inhibitor in this work, namely 2-(4-methylbenzylthio)-3-nitroimidazo [1, 2, a] pyridine (MTNI) with chemical formula $C_{15}H_{13}N_3O_2S$ and molar mass $M = 299.35\text{g/mol}$, was synthesized at the former Laboratory of Structural Organic Chemistry (LCOS) of the University Félix Houphouët Boigny of Abidjan-Cocody and its molecular structure was identified by ^1H , ^{13}C RMN spectroscopy. It is in the form of a whitish powder. The molecular structure is shown in Figure 1.

An analytical grade 37% hydrochloric acid solution from Merck was used to prepare the aqueous corrosive solution. The solution was prepared by diluting the commercial hydrochloric acid solution with distilled water. The blank was a 1 M HCl solution. The solutions prepared are of concentrations: 0.005mM; 0.01mM; 0.05mM and 0.1mM.

The 99, 9 % purity aluminium samples were in the form of a 10mm long, 20mm diameter rod.

2.2. Mass Loss Method

Mass loss measurements were carried out by total immersion of the pre-weighed aluminium sample in 100 mL capacity beakers containing 50 mL of the test solution maintained at a temperature of (298K to 323K). The samples were recovered one hour later and rinsed thoroughly with distilled water, cleaned, dried in acetone and reweighed using a balance with a sensitivity of ± 0.1 mg. All tests were performed in triplicate to ensure reliability of the results. Weight loss was considered as the difference between the initial weight and the weight after 1 h of immersion. The average values of the mass loss data were used to calculate parameters such as corrosion rate, inhibition efficiency and surface coverage using the following relationships:

$$W = \frac{\Delta m}{St} \quad (1)$$

$$EI(\%) = \frac{W_0 - W}{W_0} \times 100 \quad (2)$$

$$\theta = \frac{W_0 - W}{W_0} \quad (3)$$

Where W_0 and W are the corrosion rate in the absence and presence of the inhibitor respectively

Δm is the mass loss, S is the total surface area of the copper sample and t is the immersion time.

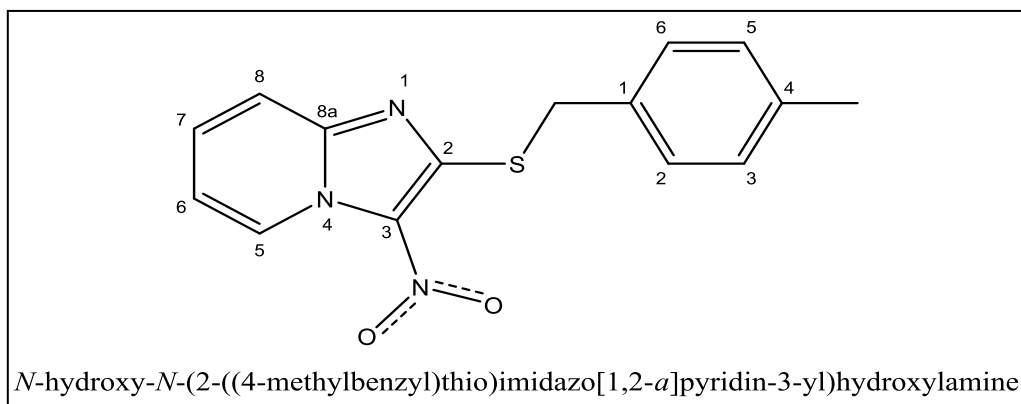


Figure 1. Molecular structure of 2-(4-methylbenzyl) thio-3-nitroimidazo [1,2-*a*]pyridine

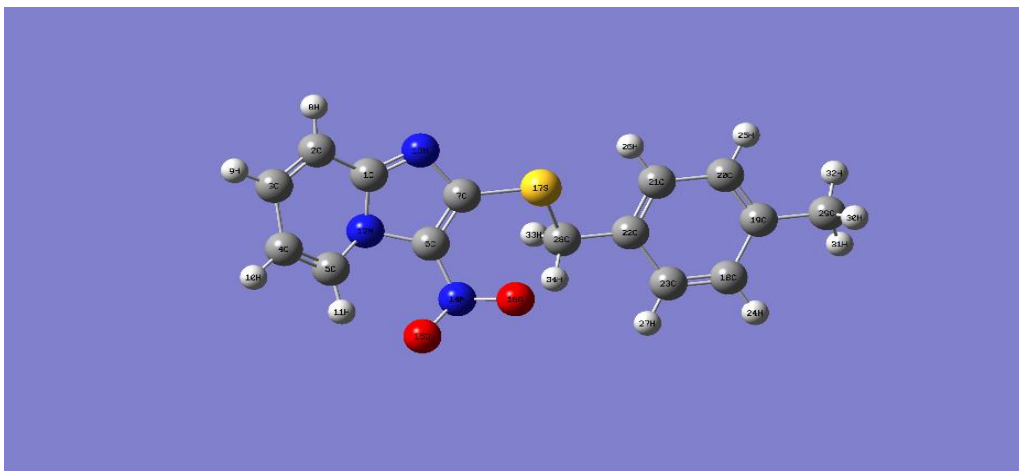


Figure 2. Optimized structure of 2-(4-methylbenzylthio)-3-nitroimidazo [1, 2, a]pyridine calculated by B3LYP/6-311G (d, p)

2.3. Quantum Chemistry Calculations

In order to explain the most important electronic effects exhibited by 2-(4-methylbenzylthio)-3-nitroimidazo [1, 2, a] pyridine (MTNI) in the inhibition of aluminium corrosion, we calculated the quantum chemical parameters. All calculations were performed in the gas phase using the Gaussian 09 software [13]. By improving the calculation method, density function theory (DFT) was widely used due to its accuracy and low computational cost to calculate a wide variety of molecular properties and provided reliable results that are consistent with the experimental data [14]. The molecular configuration of the inhibitor was geometrically optimized by this theory (DFT) with the B3LYP functional [15] (three Becke parameters with hybrid Lee-Yang-Parr correlation function) on a 6-311 G (d, p) basis set.

The basic relationship of the density functional theory of chemical reactivity is precisely, that established by Parr et al [16] which links the chemical electron potential μ_P to the first derivative of the energy with respect to the number of electrons N , and thus with the negative of the electronegativity χ :

$$\mu_P = \left(\frac{\partial E}{\partial N} \right)_{v(r)} = -\chi \quad (4)$$

The hardness η which measures both the stability and reactivity of a molecule [17] has been defined as the second derivative of the total energy E with respect to N at constant external potential $v(r)$:

$$\eta = \left(\frac{\partial^2 E}{\partial N^2} \right)_{v(r)} = \left(\frac{\partial \mu_P}{\partial N} \right)_{v(r)} \quad (5)$$

In these equations, is the chemical potential, E is the total energy, N is the number of electrons and $v(r)$ is the external potential.

According to Koopmans theorem [18], the ionization energy I can be approximated as the negative of the energy of the highest occupied molecular orbital (HOMO):

$$I = -E_{HOMO} \quad (6)$$

The negative of the lowest unoccupied molecular orbital energy (LUMO) is similarly related to the electronic affinity A as follows:

$$A = -E_{LUMO} \quad (7)$$

The electronegativity χ and the hardness η can then be written as follows:

$$\chi = \frac{I+A}{2} \quad (8)$$

$$\eta = \frac{I-A}{2} \quad (9)$$

The fraction of electrons transferred from the molecule to the metal [19] is expressed as follows:

$$\Delta N = \frac{\chi_{Cu} - \chi_{inh}}{2(\eta_{Cu} + \eta_{inh})} \quad (10)$$

The opposite of hardness is softness [20].

$$S = \left(\frac{\partial N}{\partial \mu_P} \right)_{v(r)} \quad (11)$$

The overall electrophilicity index ω introduced by Parr [21], which is a measure of the energy lowering due to maximum electron flow between the donor and acceptor, is given by:

$$\omega = \frac{\mu_P^2}{2\eta} \quad (12)$$

The local reactivity of the molecule under study can be analyzed by means of the fused Fukui indices. Condensed functions indicate the atoms in a molecule that tend to donate (nucleophilic character) or accept (electrophilic character) an electron or electron pair. The nucleophilic and electrophilic functions can be calculated using the finite difference approximation as follows:

$$f_k^+ = [q_k(N+1) - q_k(N)] \quad (13)$$

$$f_k^- = [q_k(N) - q_k(N-1)] \quad (14)$$

In equations (13) and (14), q_k is the gross charge of atom k in the molecule and N is the number of electrons.

3. Results and Discussion

3.1. Mass Loss Experiment

Mass loss data were determined at the end of a 1 hour time interval in the absence and presence of different concentrations of 2-(4-methylbenzylthio)-3-nitroimidazo [1, 2, a]pyridine (MTNI) and were used to calculate corrosion rates, inhibition efficiency and degree of surface coverage, according to equations (1 to 3).

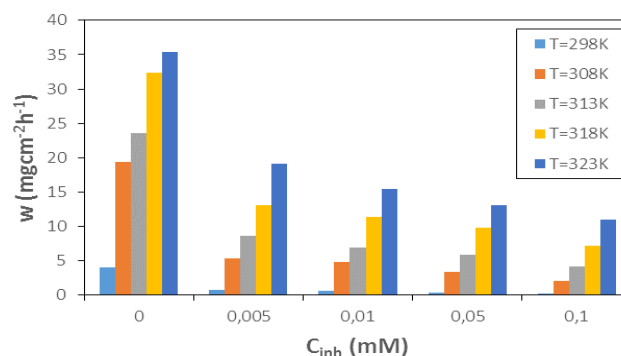


Figure 3. Corrosion rate versus MTNI concentration curve at different temperatures

Figure 3 shows the evolution of the corrosion rate with concentration and temperature respectively. Examination of Figure 3 shows that the corrosion rate increases with temperature for all concentrations and decreases with increasing inhibitor concentration. In the absence of the inhibitor, the corrosion rate is very high, which shows that the addition of MTNI to the corrosive medium delays the corrosion of aluminium. In addition, the presence of MTNI promotes the formation of a protective layer due to the adsorption of the molecule on the metal surface. This protective layer prevents the aluminium from losing sufficient electrons or undergoing strong dissolution in acid.

These results indicate that the molecule studied has a good corrosion inhibition performance of aluminium in hydrochloric acid solution.

The analysis in Figure 4 shows that the inhibitory efficiency increases with increasing inhibitor concentration but decreases with increasing temperature. This reflects the fact that the coverage of the metal surface becomes more and more important when the inhibitor concentration increases. However, it is observed that the coverage (inhibitory efficiency) decreases with increasing temperature. This behaviour could be related to a break in the adsorption-desorption equilibrium in favour of inhibitor desorption when the temperature increases.

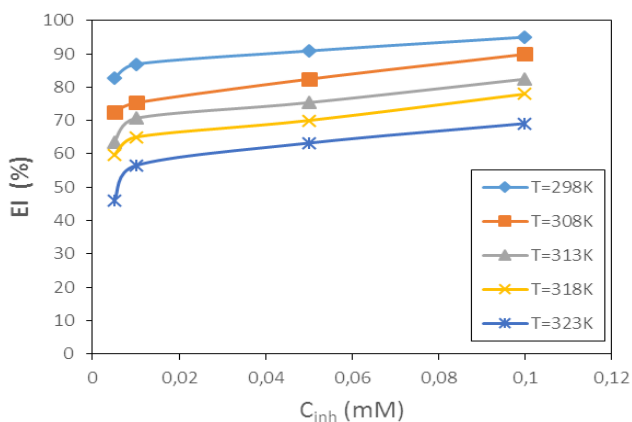


Figure 4. Inhibition efficiency versus MTNI concentration at different temperatures

3.2. Study of Adsorption Isotherms and Thermodynamic Adsorption Quantities

The study of adsorption isotherms involved in the process of inhibiting metal corrosion by organic molecules shows how these compounds attach to the surface of a metal. Indeed, the adsorption of an organic adsorbate on the metal-solution interface can be likened to a chemical reaction in which water molecules adsorbed on the metal surface are replaced by the organic molecules from the solution. It is therefore a phenomenon of substitutional adsorption [22,23] as shown by the following reaction equation:



Where $Org_{(sol)}$ and $Org_{(ads)}$ are respectively the organic molecule in solution and the organic molecule adsorbed on the metal surface, $H_2O_{(sol)}$ and $H_2O_{(ads)}$ are respectively the water molecule in solution and the water molecule adsorbed, x is the number of water molecules replaced by an organic molecule.

In this work, we tried various adsorption isotherms and selected those that best reflect the behaviour of MTNI on the aluminium surface. We have therefore chosen the Langmuir, Temkin and El-awaydy isotherms. The equations that defining these isotherms are given in Table 1.

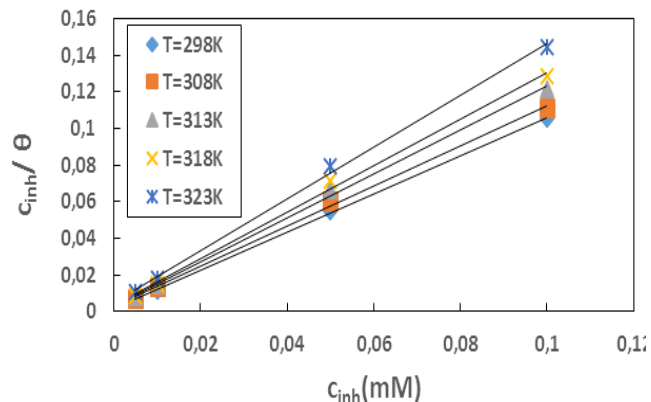


Figure 5. Langmuir adsorption isotherm plots of MTNI on aluminium in 1M HCl

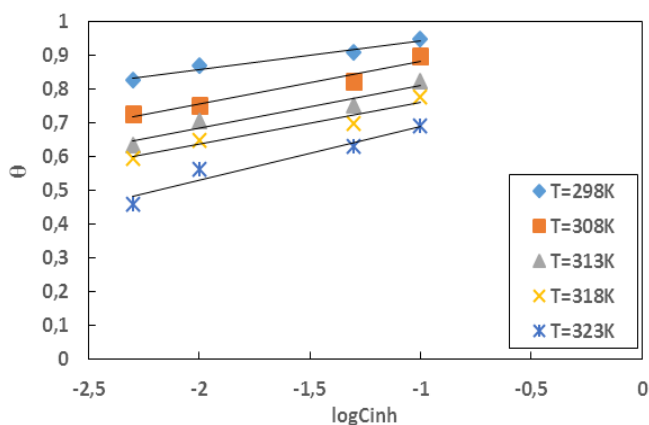


Figure 6. Temkin adsorption isotherm plots of MTNI on aluminium in 1M HCl

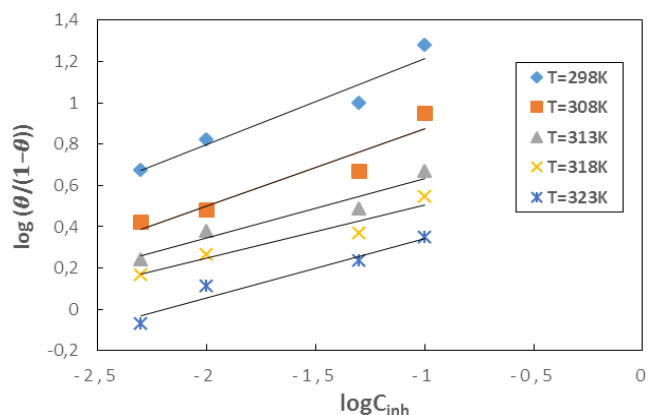


Figure 7. El-awaydy adsorption isotherm plots of MTNI on aluminium in 1M HCl

Table 1. Equations of the studied isotherms

Isotherme	Equations
Langmuir	$\frac{C_{inh}}{\theta} = \frac{1}{K_{ads}} + C_{inh}$
Temkin	$\theta = \frac{2,303}{f} [\log K_{ads} + \log C_{inh}]$
El-Awaydy	$\log \left(\frac{\theta}{1-\theta} \right) = \log K + y \log C_{inh}$

C_{inh} is the inhibitor concentration;

θ is the metal surface coverage rate;

K_{ads} is the equilibrium constant of the adsorption process;

f is an energy inhomogeneity factor of the surface;

$K_{ads} = K^{1/y}$; $1/y$ is the number of active sites occupied by an inhibitor molecule.

Figures 5, 6, 7 show the representation of these different isotherms.

All tested isotherms give straight lines as shown in Figures 5, 6 and 7.

Table 2. Isotherms parameters for different temperatures

Isotherm	T(K)	R ²	Slope	Intercept
Langmuir	298	0.999	1.0458	0.0013
	308	0.998	1.1001	0.0026
	313	0.998	1.2005	0.0029
	318	0.997	1.2686	0.0036
	323	0.999	1.4174	0.0046
Temkin	298	0.967	0.0869	1.032
	308	0.958	0.1259	1.0084
	313	0.94	0.12772	0.9402
	318	0.942	0.1252	0.9402
	323	0.939	0.1593	0.8498
El-Awady	298	0.936	0.4173	1.6334
	308	0.908	0.3736	1.2484
	313	0.932	0.2886	0.9218
	318	0.926	0.2574	0.763
	323	0.944	0.2889	0.6339

Looking at Table 2, it is clear that the correlation coefficients of the Langmuir isotherm are closer to unity than the other isotherms. Thus, this isotherm better reflects the behaviour of MTNI with respect to aluminium corrosion in 1M HCl. Nevertheless, both the Temkin and El-Awady models can be applied. For the Temkin model [24], the parameter f (where $2.303/f$ is the slope of the straight lines) having a positive value, there would be repulsive forces between the molecules adsorbed on the aluminium. In the case of the El-Awady model [25], the inverse of the slopes ($1/y$) of the straight lines obtained is greater than unity, which means that a molecule of MTNI occupies more than one site. The Langmuir adsorption model suggests that the interactions between the adsorbed particles are negligible and that each site can adsorb only one particle [26]. In this case, the adsorption of MTNI on aluminium does not strictly follow the Langmuir model; it follows the modified Langmuir isotherm or the Villamil model [27]. This model is represented by:

$$\frac{C_{inh}}{\theta} = \frac{n}{K_{ads}} + nC_{inh} \quad (15)$$

The knowledge of the appropriate adsorption isotherm allows the determination of the thermodynamic parameters of adsorption. The variation of the free energy of adsorption ΔG_{ads}^0 is calculated using the following relationship [28]:

$$\Delta G_{ads}^0 = -RT \ln(55.5K_{ads}) \quad (16)$$

Where R is the perfect gas constant, T is the absolute temperature and 55.5 is the concentration of water in mol.L^{-1} and K_{ads} is the adsorption equilibrium constant. The values of the adsorption equilibrium constant are deduced from the parameters of the modified Langmuir isotherm (straight line intercept). The other thermodynamic parameters of adsorption (adsorption enthalpy ΔH_{ads}^0 and adsorption entropy ΔS_{ads}^0) are calculated using the following relationship:

$$\Delta G_{ads}^0 = \Delta H_{ads}^0 - T \Delta S_{ads}^0 \quad (17)$$

The representation of ΔG_{ads}^0 as a function of temperature (Figure 8) leads to values of ΔH_{ads}^0 (intercept of the straight lines) and ΔS_{ads}^0 (the slope of the straight line). The different thermodynamic adsorption parameters are recorded in Table 3.

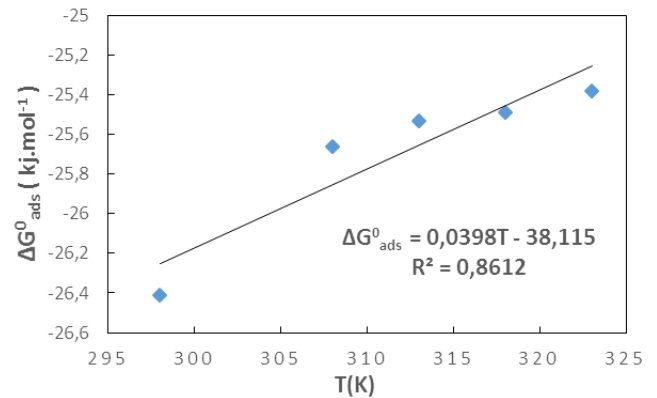


Figure 8. Variation of ΔG_{ads}^0 versus temperature

Table 3. K_{ads} values and thermodynamic adsorption parameters for MTNI

T (K)	K_{ads}	ΔG_{ads}^0 (kJ.mol^{-1})	ΔH_{ads}^0 (kJ mol^{-1})	ΔS_{ads}^0 ($\text{J mol}^{-1}\text{K}^{-1}$)
303	769,23	-26,41	-38,115	-39,8
308	384,61	-25,66		
313	344,83	-25,53		
318	277,78	-25,49		
323	217,39	-25,38		

Negative values of ΔG_{ads}^0 indicate the stability of the adsorbed layer on the aluminium surface and the spontaneity of the adsorption process [29]. According to the literature [30], a value of ΔG_{ads}^0 lower than -40 kJ.mol^{-1} would indicate a chemical adsorption process (chemisorption) whereas a value higher than -20 kJ.mol^{-1} would indicate a physical adsorption process (physisorption). For values between -40 kJ.mol^{-1} and -20 kJ.mol^{-1} , both types of adsorption would exist. In view of the values contained in Table 3, we can deduce that the adsorption of MTNI on aluminium takes place according to the two adsorption modes (physisorption and chemisorption). The negative sign of ΔH_{ads}^0 reflects the exothermic character of the adsorption of the molecule on aluminium. If the value of

ΔS_{ads}^0 is negative, this reflects a decrease in disorder during the adsorption of the inhibitor. An increase in disorder [31] would be related to the desorption of water molecules, whereas a decrease could be related to the weakening of the adsorption force.

In order to correctly justify the adsorption mode of the studied molecule, we used the Adejo-Ekwenchi isotherm [32]. Indeed, this isotherm allows us to know the adsorption mode of an organic compound. This model is based on the following equation:

$$\log \frac{1}{1-\theta} = \log K_{AE} + b \log C_{inh} \quad (18)$$

Where and are isotherm parameters.

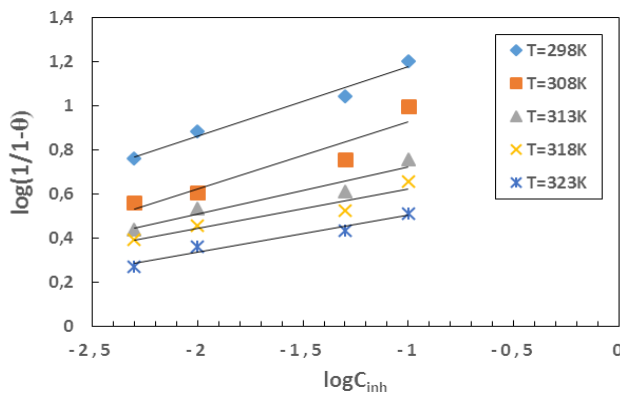


Figure 9. Adejo-Ekwenchi isotherm plots of MTNI on aluminium in 1M HCl

The parameters of this isotherm are given in Table 4

Table 4. Parameters of the Adejo-Ekwenchi isotherm

T(K)	b	K_{AE}	R^2
298	0.3151	31,017	0,974
308	0.3057	17,159	0,891
313	0.2126	8606	0,924
318	0.1777	6,314	0,911
323	0.1679	4,682	0,957

As shown in Table 4, the b and K_{AE} parameters decrease with increasing temperature, indicating that the adsorption of MTNI on aluminium is dominated by physisorption [33].

3.3. Effect of Temperature and Activation Parameters on the Corrosion Process

The effect of temperature on corrosion and its inhibition process for aluminium in 1M in the absence and presence of different concentrations of MTNI at different temperatures ranging from 298K to 323K was evaluated.

The temperature dependence of the corrosion rate can be considered as an Arrhenius-type process, whose rate is given by [34]

$$\log W = \log A - \frac{E_a}{2,303RT} \quad (19)$$

Where W is the corrosion rate, R is the perfect gas constant, A is the frequency factor.

The curve of $\log W$ versus $1/T$ is given in Figure 10.

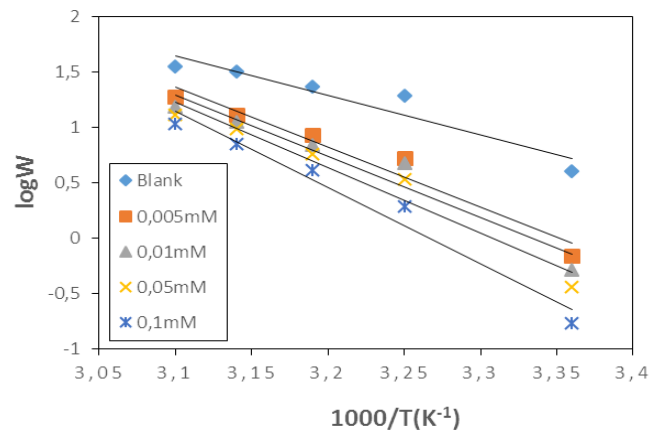


Figure 10. Arrhenius plots for aluminium in 1M HCl in the absence and presence of MTNI

The Arrhenius plots allow the deduction of activation energy values using the slopes of the linear lines. All values obtained are listed in Table 5. The effect of temperature is also verified by determining the change in activation enthalpy ΔH_a^* and the change in activation entropy ΔS_a^* using the equation of transition states:

$$W = \frac{R.T}{\aleph.h} \exp\left(\frac{\Delta S_a^*}{R}\right) \cdot \exp\left(-\frac{\Delta H_a^*}{R.T}\right) \quad (20)$$

This relationship leads to the following relationship:

$$\log\left(\frac{W}{T}\right) = \log\left(\frac{R}{\aleph.h}\right) + \frac{\Delta S_a^*}{2,3.R} - \frac{\Delta H_a^*}{2,3.R.T} \quad (21)$$

Where h is Planck's constant and \aleph is Avogadro's constant, E_a activation energy, ΔH_a^* activation enthalpy variation and ΔS_a^* activation entropy variation.

The representation of $\log\left(\frac{W}{T}\right)$ as a function of $1/T$ is given in Figure 11

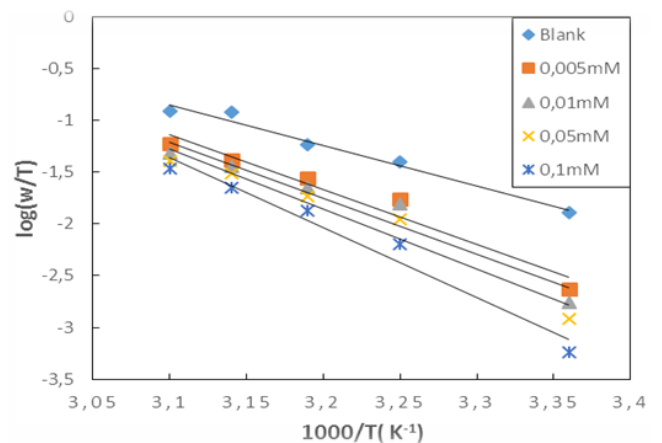


Figure 11. Arrhenius plots for aluminium in 1M HCl in the absence and with different concentrations of MTNI

The parameters ΔH_a^* and ΔS_a^* are calculated from the slope $\left(-\frac{\Delta H_a^*}{2,3.R.T}\right)$ and intercept $\left(\log\left(\frac{R}{\aleph.h}\right) + \frac{\Delta S_a^*}{2,3.R}\right)$ of the straight lines obtained respectively. The values obtained are recorded in Table 5.

Table 5. Thermodynamic values of aluminium dissolution in 1M HCl without and with different concentrations of MTNI

Concentration (mM)	E_a ($kJ.mol^{-1}$)	ΔH_a^* ($kJ.mol^{-1}$)	ΔS_a^* ($J.mol^{-1}.K^{-1}$)
0	68.85	75.14	19.06
0.005 mM	103.46	100.99	93.58
0.01 mM	106.02	103.49	100
0.05 mM	113.694	111.19	122.66
0.1 mM	131.97	129.51	177.93

The values of the activation energies in the presence of the molecule are higher than the value obtained without the molecule ($C_{inh} = 0$). Thus the activation mechanism is influenced by physisorption. The activation energy increases when the inhibitor concentration increases, thus favouring the formation of electrostatic bonds, which are weak.

The positive signs of the activation enthalpy variations (ΔH_a^*) reflect the endothermic nature of the aluminium dissolution process. The values of the activation entropy variations ΔS_a^* are all positive, reflecting an increase in disorder during the dissolution of aluminium which could be the reason for the decrease in inhibitory efficiency when the temperature increases.

3.4. Molecular Descriptor Parameters

In this study the quantum parameters were calculated using the descriptors of the conceptual density functional theory (DFT) which are very important to explain the reactivity of the molecule. In general, this theory allows to confirm the experimental results. The values of the different descriptor parameters of the molecule are reported in Table 6.

Table 6. MTNI descriptor parameters obtained from B3LYP/6-311G (d, p)

Paramètres	Valeurs
E_{LUMO} (eV)	-2,5935
E_{HOMO} (eV)	-6,3966
energy gap ΔE (eV)	3,8031
Dipole moment μ (D)	2,3241
Ionization energy I (eV)	6,3966
Electron affinity A (eV)	2,5935
Electronegativity χ (eV)	4,4950
Hardness η (eV)	1,9016
Softness σ (eV) ⁻¹	0,5259
Fraction of transferred electrons ΔN	-0,0565
Electrophilicity index ω	5,3128
total Energy E_T (Ha)	-1292,3

The ability of a molecule to bond to a metal surface depends on both the E_{LUMO} (energy of the lowest unoccupied orbital) and the HOMO (energy of the highest occupied orbital). The low E_{LUMO} value (-2.593 eV) of

2-(4-methylbenzyl) thio)-3-nitroimidazo [1, 2, a]pyridine (MTNI) shows the ability of the molecule to accept electrons from a given system. The energy E_{HOMO} is the overall reactivity parameter of molecules associated with the ability to donate electrons. A high value of E_{HOMO} for a molecule [35] would favour its tendency to donate electrons to a suitable acceptor with a vacant low energy orbital. The value of E_{HOMO} (- 6.397 eV) in the case of our molecule could justify the high values of inhibitory efficiency of the molecule towards the corrosion of aluminium in hydrochloric acid medium. The value of the energy gap $\Delta E = E_{LUMO} - E_{HOMO}$ is also an important reactivity parameter for organic molecules. Low values of ΔE would favour exchanges between the molecules and the metal. It has been proven [35] that molecules with ΔE values of the order of 5eV are good inhibitors. In our case the low value of ΔE (3.8031eV) would justify the high inhibitory efficiencies obtained. The negative value of ΔN shows that the molecule tends to receive electrons from aluminium.

The overall softness (S) and the overall hardness (η) are also important reactivity parameters that give information on the likely abilities of a molecule to interact with a metal surface. A good inhibitor has a high softness value and a low hardness value. The molecule has a low hardness value ($\eta=1.9016$ eV) and a high softness (0.5259 (eV)⁻¹). These values are in agreement with the experimental results.

The dipole moment (μ), which is related to the distribution of electronic charges in the molecule, is also an important parameter that reflects the ability of the molecule to adsorb to the surface of a metal. According to certain authors [36,37], the ability of a molecule to adsorb to the surface of a metal is all the greater as its dipole moment is high. In our case, the value of this parameter is high ($\mu=2.3241$ Debye) which could explain the high adsorption rates and therefore the high values of inhibitory efficiency of the molecule.

The ionization energy (I) is an indispensable descriptor of the chemical reactivity of atoms and molecules. A high ionization energy [38] indicates that the molecule is stable and inert to any chemical reaction, whereas a low ionization energy indicates the high reactivity of atoms and molecules. The low ionization energy of the inhibitor indicates its high inhibitory efficiency.

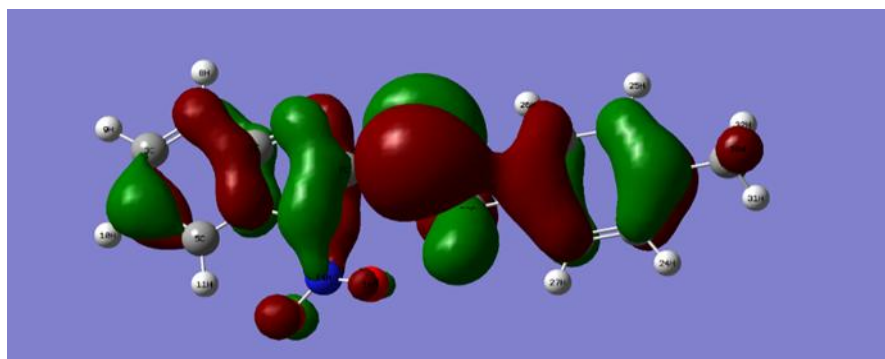
The electrophilicity index (ω) measures the ability of a chemical species to accept electrons. A high value of ω [39] describes a good electrophile, while a low value of ω describes a good nucleophile. This index of overall reactivity measures the stabilization of energy when the system acquires additional electron charge from the environment. The value of the electrophilicity index (5.3128 eV) for the molecule is high, showing its ability to receive electrons from the metal.

The values of the Fukui function and the local softness of the electrophilic and nucleophilic attack sites are collected in Table 7.

Table 7. Values of the Fukui function, natural loads and the dual descriptor

Atomes	q (N+1)	q(N)	q (N-1)	f+	f-	$\Delta f(r)$
1 C	0,023626	0,456446	0,108768	-0,43282	0,347678	-0,780498
2 C	0,000097	-0,080047	-0,056368	0,080144	-0,023679	0,103823
3 C	0,004129	-0,075437	0,116789	0,079566	-0,192226	0,271792
4 C	0,03191	-0,12501	0,038274	0,15692	-0,163284	0,320204
5 C	-0,014645	0,090448	-0,005774	-0,105093	0,096222	-0,201315
6 C	0,056361	0,442387	-0,029288	-0,386026	0,471675	-0,857701
7 C	0,002352	0,017552	0,167907	-0,0152	-0,150355	0,135155
8 H	-0,000067	0,128691	0,002	-0,128758	0,126691	-0,255449
9 H	-0,000168	0,11473	-0,006431	-0,114898	0,121161	-0,236059
10 H	-0,001285	0,112343	-0,002635	-0,113628	0,114978	-0,228606
11 H	0,000414	0,189814	-0,000964	-0,1894	0,190778	-0,380178
12 N	0,013178	-0,503076	0,096518	0,516254	-0,599594	1,115848
13 N	0,004954	-0,498432	-0,062102	0,503386	-0,43633	0,939716
14 N	-0,006559	0,111037	0,220595	-0,117596	-0,109558	-0,008038
15 O	0,033709	-0,345077	0,178745	0,378786	-0,523822	0,902608
16 O	-0,007208	-0,321634	0,187955	0,314426	-0,509589	0,824015
17 S	0,460552	0,273908	0,014713	0,186644	0,259195	-0,072551
18 C	-0,041999	-0,107007	-0,002397	0,065008	-0,10461	0,169618
19 C	0,117171	0,099149	0,00549	0,018022	0,093659	-0,075637
20 C	0,147792	-0,133017	0,001631	0,280809	-0,134648	0,415457
21 C	-0,062714	-0,128348	-0,000441	0,065634	-0,127907	0,193541
22 C	0,141126	0,076402	0,003886	0,064724	0,072516	-0,007792
23 C	0,082906	-0,097405	0,005954	0,180311	-0,103359	0,28367
24 H	0,000918	0,088309	0,000101	-0,087391	0,088208	-0,175599
25 H	-0,006108	0,085009	-0,000048	-0,091117	0,085057	-0,176174
26 H	0,00157	0,113997	0,000012	-0,112427	0,113985	-0,226412
27 H	-0,003513	0,093223	-0,000353	-0,096736	0,093576	-0,190312
28 C	-0,027861	-0,431586	0,016209	0,403725	-0,447795	0,85152
29 C	-0,003162	-0,374772	-0,000489	0,37161	-0,374283	0,745893
30 H	0,013281	0,133267	0,000389	-0,119986	0,132878	-0,252864
31 H	0,003174	0,116341	0,000095	-0,113167	0,116246	-0,229413
32 H	0,002834	0,119468	0,000202	-0,116634	0,119266	-0,2359
33 H	0,00714	0,158991	0,001611	-0,151851	0,15738	-0,309231
34 H	0,026095	0,199333	-0,000543	-0,173238	0,199876	-0,373114

Figures 12 and 13 below give us the HOMO and LUMO densities of our molecule.

**Figure 12.** HOMO density of the inhibitor at B3LYP/6-311G (d, p)

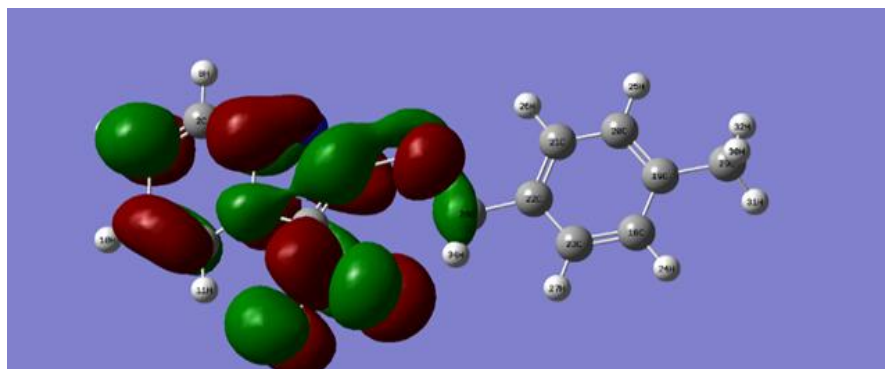


Figure 13. LOMO density of the inhibitor at B3LYP/6-311G (d, p)

In DFT, the so-called Fukui functions are advocated as reactivity descriptors to identify the most reactive sites for electrophilic or nucleophilic reactions in a molecule.

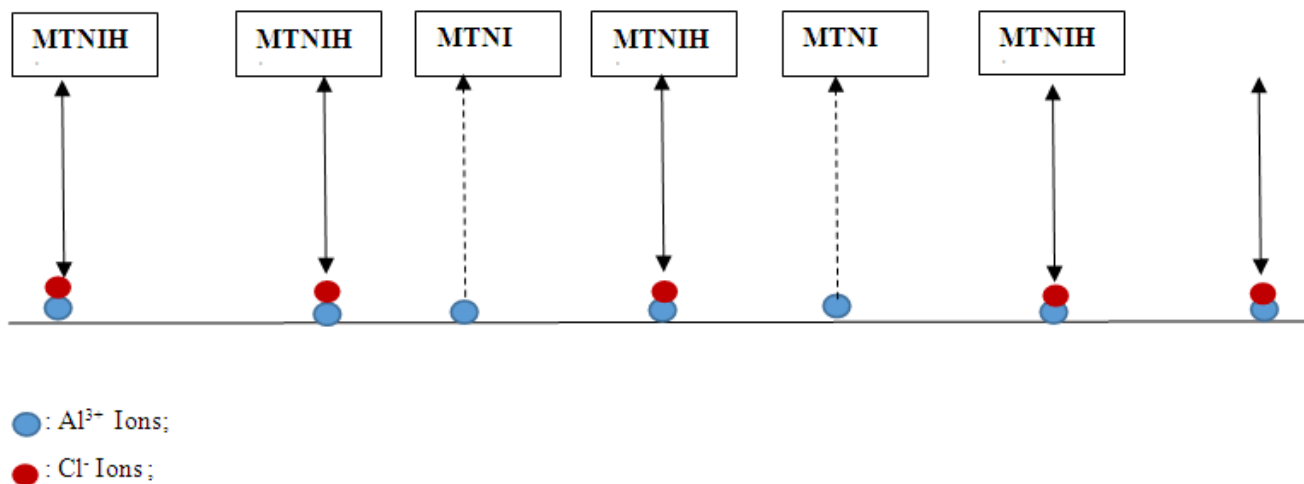
The most common expression is [40]:

$$f(\vec{r}) = \left(\frac{\partial \rho(\vec{r})}{\partial N} \right)_{v(\vec{r})} \quad (22)$$

They reflect the change in electron density at a point relative to a change in the number of electrons, under a constant external potential. Molecular properties are often associated with a certain point in space. It is then necessary to identify an atom in the molecule. The difficulty is that there is not yet an operator [41] that, acting on the wave function or the electron density, can perform a division of space into atomic pools. Despite this fundamental problem, Fukui functions are often condensed to an atomic resolution. These condensed Fukui functions (equations (13) and (14)) are, in the context of the variational approach to chemical reactivity, more informative indicators of molecular site reactivity than the Fukui functions (equation (22)). From the

Scheme of the mechanism

Schéma du mécanisme



The double arrows indicate electrostatic interactions (physisorption) and the arrows with interrupted supports

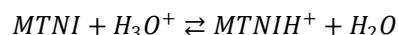
values of the calculated Fukui and local softness functions, it can be seen in Table 5 that nucleophilic attacks take place around the C6 carbon atom, while electrophilic attacks are located around the N12 nitrogen atom.

3.5. Mechanism of Corrosion Inhibition of Aluminum in HCl Medium by 2-(4-methylbenzylthio)-3-nitroimidazo [1, 2, a]pyridine (MTNI)

The experimental and theoretical results show that: MTNI cannot supply electrons to aluminum ($\Delta N < 0$)

MTNI can receive electrons from aluminium ($\omega = 5.3128$ eV)

In the presence of the hydronium ion H_3O^+



$MTNIH^+$ reacts with Cl⁻ ions attached to Al⁺³ ions

On some sites, the aluminium gives up electrons to the molecule (on the electrophilic part of the molecule N(13).

indicate the contribution of electrons to the molecule and formation of the TTNIAI complex.

4. Conclusions

The mass loss technique and the DFT method were used to evaluate the corrosion inhibition of aluminium by 2-(4-methylbenzyl) thio)-3-nitroimidazo [1,2,a] pyridine (MTNI) in 1M HCl.

The following conclusions can be drawn from this study:

MTNI acts as a good corrosion inhibitor for aluminium in 1M hydrochloric acid.

The inhibition efficiency is concentration and temperature dependent.

MTNI adsorbs to aluminium according to the modified Langmuir isotherm.

The calculated thermodynamic parameters related to adsorption and activation show the existence of two types of adsorption (physisorption is preponderant).

The chemical quantum parameters confirm the inhibition efficiency of MTNI.

Condensed Fukui functions show the nucleophilic and electrophilic sites in the molecule.

REFERENCES

- [1] S. Ambat, E. S. Dwarakadasa, Studies on the influence of chloride ion and pH on the electrochemical behaviour of aluminium alloys 8090 and 2014, *J. Appl. Electrochem.*, 1994, 24, 911-616.
- [2] Amit Kumar Dewangan, Yeestdev Dewangan, Dakeshwar Kumar Verma and Chandrabhan Verma, Synthetic environment-friendly corrosion inhibitors, Environmentally Sustainable Corrosion Inhibitors Fundamentals and Industrial Applications (2022) Pages 71-95. <https://doi.org/10.1016/B978-0-323-85405-4.00020-3>.
- [3] S. Sankarapavinasam, F. Pushpanden, M. F. Ahmed, *Trosyl-hydrazine, 4-nitrobenzoyl-hydrazine and terephthalyl-hydrazine as inhibitors for the corrosion of copper and aluminium in sulphuric acid*, *J. Applied Electrochem.*, 1991, 21, 625-631.
- [4] G. K. Gomma, M. H. Wahdan, *Schiff bases as corrosion inhibitors for aluminium in hydrochloric acid solution*, *Mater. Phys.*, 1995, 39, 209-213.
- [5] A. Yurt, S. Ulutas, H. Dal, *Appl. Surf. Sci., Electrochemical and Theoretical investigation on the corrosion of aluminium in acidic solution containing Schiff bases*, 2006, 253, 919-925.
- [6] J. Obot, N. O. Obi-Egbedi, S. A. Umoren, *Antifungal drugs as corrosion inhibitors for aluminium in 0,1M HCl*, *Corros. Sci.*, 2009, 51, 1868-1875.
- [7] M. Abdallah, *Antibacterial drugs as corrosion inhibitors for corrosion of aluminium in hydrochloric acid solution*, *Corros. Sci.*, 2004, 46, 1981-1996.
- [8] S. M. Tamborim, S. L. P. Dias, S. N. Silva, L. F. P. Dick, D. S. Azambuja, *Preparation and electrochemical characterization of amoxicillin-doped cellulose acetate films for AA 2024-T3 aluminium alloy coatings*, *Corros. Sci.*, 2011, 53, 1571-1580.
- [9] A. S. Fouda, A. A. Al-Sarawy, F. Sh. Ahmed, H. M. El-Abbasy, *Corrosion inhibition of aluminium 6063, using some pharmaceutical compounds*, *Corros. Sci.*, 2009, 51, 485-492.
- [10] I. B. Obot, S. A. Umoren, N. O. Obi-Egbedi, *Corrosion inhibition and adsorption behaviour for aluminium by extract of Aningeric robusta in HCl solution: synergistic effect of iodide ions*, *J. Mater. Environ. Sci.*, 2011, 2, 60-71.
- [11] I. J. Alinnor, P.M. Ejikeme, *Corrosion inhibition of aluminium in acidic medium by different extracts of Ocimum gratissimum*, *American Chemical Journal*, 2012, 2, 122-135.
- [12] S. I. Al-Saedi, G. M. Al-Semani, R. Almufarij, *Electrochemical investigations on the corrosion inhibition of aluminium by green leafy vegetables in 1M HCl*, *Life Science Journal*, 2016, 13, 100-105.
- [13] M. J. Frisch, G. W. Trucks, H. B. Schlegel, G. E. Scuseria, M. A. Robb, J. R. Cheeseman, G. Scalmani, V. Barone, B. Mennucci, G. A. Petersson, H. Nakatsuji, M. Caricato, X. Li, H. P. Hratchian, A. F. Izmaylov, J. Bloino, G. Zheng, J. L. Sonnenberg, M. Hada, M. Ehara, K. Toyota, R. Fukuda, J. Hasegawa, M. Ishida, T. Nakajima, Y. Honda, O. Kitao, H. Nakai, T. Vreven, J. A. Montgomery, Jr., J. E. Peralta, F. Ogliaro, M. Bearpark, J. J. Heyd, E. Brothers, K. N. Kudin, V. N. Staroverov, R. Kobayashi, J. Normand, K. Raghavachari, A. Rendell, J. C. Burant, S. S. Iyengar, J. Tomasi, M. Cossi, N. Rega, J. M. Millam, M. Klene, J. E. Knox, J. B. Cross, V. Bakken, C. Adamo, J. Jaramillo, R. Gomperts, R. E. Stratmann, O. Yazyev, A. J. Austin, R. Cammi, C. Pomelli, J. W. Ochterski, R. L. Martin, K. Morokuma, V. G. Zakrzewski, G. A. Voth, P. Salvador, J. J. Dannenberg, S. Dapprich, A. D. Daniels, Ö. Farkas, J. B. Foresman, J. V. Ortiz, J. Cioslowski and A. D. J. Fox, Gaussian, Inc., Wallingford, (2009), 09.
- [14] Benhiba F., Serrar H., Hsissou R., Guenbour A., Bellaouchou A., Tabyaoui M., Boukhris S., Oudda H., Warad I. and Zarrouk A., 2020, Tetrahydropyrimido-Triazepine derivatives as anti-corrosion additives for acid corrosion: Chemical, electrochemical, surface and theoretical studies. *Chemical Physics Letters* 743, 137181.
- [15] C. Lee, W. Yang, R.G. Parr, 1988, Development of the Colle-Salvetti correlation-energy formula into a functional of the electron density, *Physical Review B*, 37,785-789.
- [16] R G Parr; R A Donnelly; M Levy; W E Palke, *J. Chem. Phys.*, 1978, 68, 3801-3807.
- [17] T Koopmans, *Physica (Elsevier)*, 1934, 1, 104-113.
- [18] R G Pearson, *Inorg. Chem.*, 1988, 27, 734-740.
- [19] WYang and R G Parr, *Proc. Natl. Acad. Sci. U.S.A.*, 1985, 82, 6723 - 6726.
- [20] R G Parr; L Szentpaly and S Liu, *J. Am. Chem. Soc.*, 1999, 121, 1922-1924.
- [21] E A Essien; S A Umoren; E E Essien and A P Udoh, *J. Mater. Environ. Sci.*, 2012, 3, 477 - 484.
- [22] J. Aljourani, K. Raessi, M. A. Golozar, Benzimidazole and its derivatives as corrosion inhibitors for mild steel in 1M HCl, *Corros. Sci.*, 2006, 51, 1836-1843.
- [23] J. O' M. Bockris, D. Drazic, The kinetics of deposition and dissolution of iron: Effect of alloying impurities, *Electrochem. Acta*, 1962, 7, 293-313.

- [24] M. I. Temkin, 1941, Adsorption equilibrium and process Kinetics on inhomogeneous surfaces with interaction between adsorbed molecules, *Zh. Fiz. Khim.*, 15(3), 296-332.
- [25] Y. A. El Awady, A. I. Ahmed, 1985, Effect of temperature and inhibitors on the corrosion of aluminium in 2N HCl solution, A kinetic study, *Journal of Indian Chemistry*, 24, 601-606.
- [26] Irving Langmuir, 1916, the constitution and fundamental properties of solids and liquids, *Journal of the American Chemical Society*, 38(11), 2221-2295.
- [27] Villamil R F. V., Corio P., Rubín J. C., Agostinho S. M. L., 1999, Effect of sodium dodecylsulfate on copper corrosion in sulfuric acid media in the absence and presence of benzotriazole, *Journal of Electroanalytical Chemistry*, 472, 112-116.
- [28] Vashi R. T., Champaneri V. A., 1997, Toluidines as corrosion inhibitors for zinc in sulphamic acid *Indian Journal of Chemical Technology*, 4, 180-184.
- [29] Noor E.A., Al-Moubaraki A.H., 2008, Thermodynamic study of metal corrosion and inhibitor adsorption processes in mild steel/1-methyl-4[4(-X)-styryl pyridinium iodides/hydrochloric acid systems, *Materials Chemistry and Physics*, 110, 145-154.
- [30] AFNOR, *Corrosion des métaux et alliages: terme principaux et définition*, Paris, 2000.
- [31] I.N. Putilova, S. A. Balezin, V. P. Barannik, *Metallic Corrosion Inhibitors*, Pergamon Press, Oxford, 1960, 30.
- [32] S O Adejo; M. M Ekwenchi. IOSR., 2014, Resolution of adsorption characterisation ambiguity through the Adejo-Ekwenchi adsorption isotherm: a case study of leaf extract of *Hyptis suaveolens* as green corrosion inhibitor of corrosion of mild steel in 2 M HCl *Journal of Emerging Trends in Engineering and Applied Sciences*, 8(5), 201 – 205.
- [33] Adejo, Sylvester O. Proposing a new empirical adsorption isotherm known as Adejo-Ekwenchi isotherm. *Journal of Applied Chemistry*, 2014, vol. 6, no 5, p. 66-71.
- [34] Li, Y.; Zhao, P.; Liang, Q.; Hou, B., 2005, Berberine as a natural source inhibitor for mild steel in 1 M H₂SO₄, *Applied Surface Science*, 252(5), 1245-1253.
- [35] P. M. Niamien, F. K. Essy, A. Trokourey, A. Yapi, H. K. Aka, D. Diabaté, Correlation between the molecular structure and the inhibiting effect of some Benzimidazole derivatives.
- [36] H. B. Michaelson, The work function of the elements and its periodicity, *J. Appl. Phys.* 1977, 48, 4729-4733.
- [37] E. E. Ebenso, D. A. Isabirye, N. O. Eddy, Adsorption and Quantum Chemical Studies on the inhibition potentials of Some Thiosemicarbazides for the corrosion of Mild steel in Acidic Medium, *Int. J. Mol. Sci.*, 2010, 11, 2473-2498.
- [38] Chakraborty T and Ghosh D C Computation of the atomic radii through the conjoint action of the effective nuclear charge and the ionization energy, *Mol. Phys.*, 2010, 108(16), 2081-2092. *Materials Chemistry and Physics*, 2012, 136, 59-65.
- [39] R. G. Parr, L. Szentpaly, S. Liu, *Electrophilicity index*, *J. Am. Chem. Soc.*, 1999, 121(9) 1922-1924.
- [40] R G Parr and W Yang, *Density Functional Theory of Atoms and Molecules*, Oxford University Press: Oxford, U.K., 1989.
- [41] P Bultinck; R Carbo-Dorca and W Langenaeker, *Journal of Chemical Physics*, 2003, 118, 4349-4356.